INFLUENCE OF STRAND DISPERSION METHOD ON MECHANICAL PROPERTIES OF HOLLOW-S-SHAPED MEMBER MADE OF RANDOMLY-ORIENTATED CFRTP STRANDS

Michinobu Fujita[1], Yuto Nakashima[1] and Jun Takahashi[1]

[1] The University of Tokyo, Department of Systems Innovation, School of Engineering,
7-3-1 Hongo, Bunkyo-ku, Tokyo 113-8656, JAPAN
Email: fujita-michinobu@cfrtp.t.u-tokyo.ac.jp
Web page: http://j-t.o.oo7.jp/index-e.html

Keywords: FEM analysis, discontinuous carbon fiber reinforced thermoplastics, hollow S-shaped member

ABSTRACT

In order to reduce CO_2 emissions, the improvement of automobile fuel economy is important. As a solution, researches to applying carbon fiber reinforced plastics (CFRP), which are super-lightweight materials, to automobiles has been actively conducted in recent years. In our laboratory, we focused on chopped carbon fiber tape reinforced thermoplastics (CTT), which are a type of randomly-oriented strands (ROS) as moldable materials of automotive structure having complex shape. However, the orientation of chopped carbon fiber tape depending on the tape dispersion method causes a difference in mechanical properties and their scatters of the products. In this study, the influence of strand dispersion method on mechanical properties of the hollow S-shaped member was investigated with compression tests and finite element analysis (FEA).

1. INTRODUCTION

Weight reduction of automobiles is effective to improve both driving performance and fuel efficiency. CFRP have been expected as ultra-lightweight structural materials, but they have hardly been applied to commercial vehicles. In our laboratory, we are studying an application of topological analysis to automobile frame structures [1]. In order to apply CFRP to automobiles, design method development is important. In addition, it is also an important factor to have mass-productivity with designed mechanical properties and designed shapes. In automotive parts, there are not only straight simple shapes but also complicated shapes with curvature, and in the case of continuous carbon fiber reinforced composites wrinkles are generated in press-forming at curvature parts. Because the wrinkles impair fiber linearity and work as a starting point of fracture, the expected structural stiffness and strength calculated by standard mechanical test results do not appear. Therefore, in order to solve the formability of continuous CFRP, many researches on ROS has been carried out [2-4]. Especially we focused on chopped carbon fiber tape reinforced thermoplastics (CTT), which are a type of ROS with randomly-oriented thermoplastic prepreg. A previous study reported that an application of thin-ply to CTT makes the mechanical properties greater and their scatter lower [5]. CTT is classified into bulk molding CTT (BM-CTT) and sheet molding CTT (SM-CTT) according to the strand dispersion method. In this study, we investigated the influence of strand dispersion method on mechanical properties of hollow S-shaped members derived from an automobile frame structure.

2. EXPERIMENTAL

2.1 Materials and Hollow S-shaped Member preparation

Chopped unidirectional prepreg tapes used in this study were prepared at Industrial Technology Center of Fukui Prefecture. Carbon fibers (TR50S) and Polyamide 6 (DAIAMIRON® C) were provided by Mitsubishi Chemical Co. The tape thickness was 44 μm, length was 19 mm, width was 5 mm, and the volume fraction of carbon fiber was 54%.

Figure 1 shows the scheme of the hollow S-shaped member preparation method for each dispersion method. BM-CTT was manufactured by the following procedure. 1) Chopped tapes were put into the molding die directly. 2) Compression molding. As mentioned above, BM-CTT has the advantage that the process is simple because the chopped tapes are just put into the mold directly. On the other hand, because heat & cool molding is necessary, there is a disadvantage that it is unsuitable for mass-production.

Next, SM-CTT was manufactured by the following procedure. 1) Chopped tapes were dispersed. 2) Dispersed tapes were fixed by heat and pressure, and an intermediate sheet was prepared. 3) The intermediate sheets were put into the molding die and compressed. In the case of SM-CTT, although the process is complicated, stamp molding can be adopted, which has the advantage of short production time.

Figure 2 shows the thickness measurement points and the measurement results. In order to measure the thickness, digimatic micrometer (MDE-25MX, Mitutoyo Corporation) was used for flanges (1^{st} and 5^{th} rows in Figure 2 upper left), and dial caliper gauge (LA-8, Ozaki mfg. co. ltd.) was used for the rest. As shown in Figure 2, the average thickness was about 2.45 mm, which was 2% thinner than the designed thickness. The variation for each measurement point was in the range of +2% to -6%. For FEA, it was modeled as uniformly 2.5 mm.

Figure 3 shows the model of the hollow S-shaped member. The molded hat section members were bonded with a methacrylate adhesive (MA310, ITW Plexus) to prepare a hollow S-shaped member. The thickness of the adhesive was adjusted to 1 mm with spacers. In order not to consider breakage of adhesive part in FEA, both sides of flanges were riveted. And then, the all edges were trimmed by machining. Before the compression test, the members were dried at 50° C for 8 hours and conditioned at 23°C, 50%RH for 8 hours.

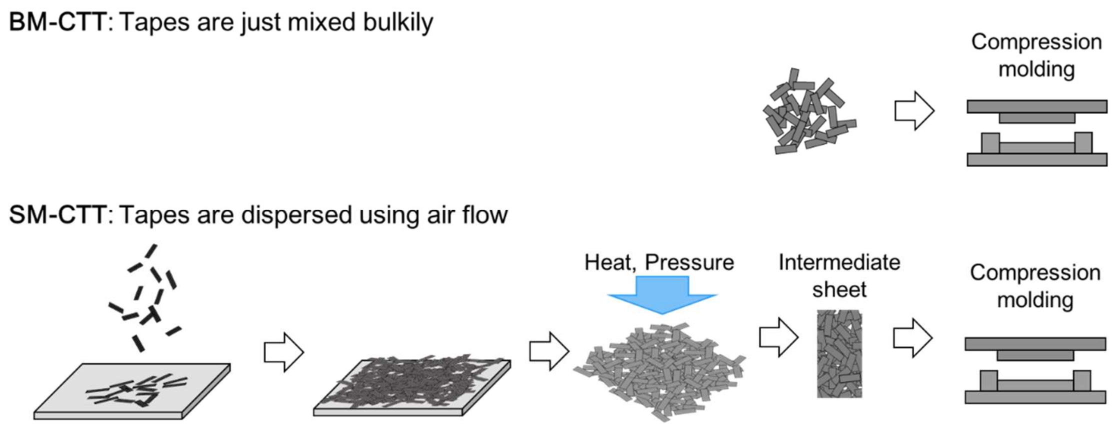

Figure 1: Schemes of BM-CTT and SM-CTT preparation.

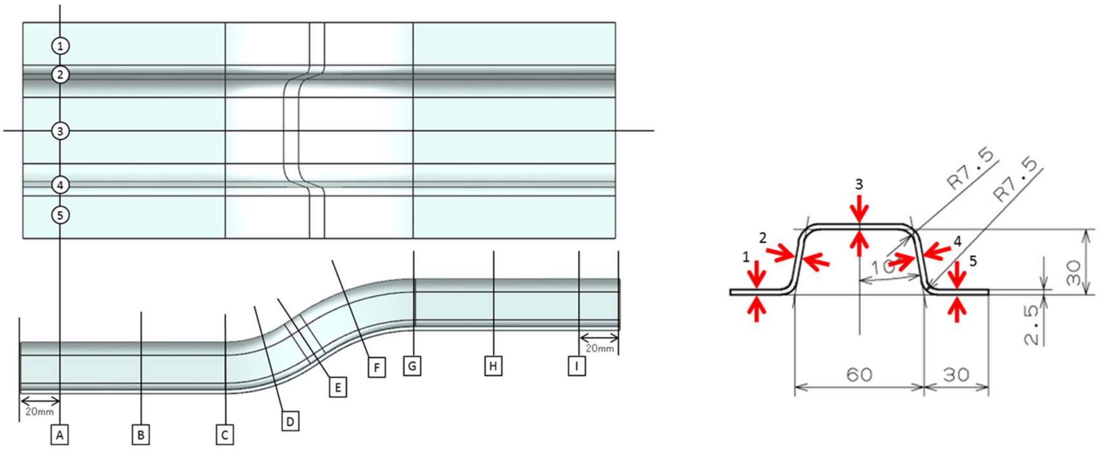

BM-CTT (n=9)											
	A	B	C	D	E	F	G	H	I	average	standard deviation
1	2.482	2.465	2.478	2.502	2.498	2.483	2.478	2.481	2.504	2.453	0.046
2	2.438	2.430	2.412	2.418	2.411	2.380	2.366	2.352	2.357		
3	2.446	2.451	2.474	2.453	2.479	2.499	2.441	2.477	2.452		
4	2.482	2.500	2.472	2.472	2.468	2.493	2.517	2.548	2.534		
5	2.380	2.380	2.385	2.438	2.480	2.463	2.407	2.420	2.448		

SM-CTT (n=7)											
	A	B	C	D	E	F	G	H	I	average	standard deviation
1	2.535	2.516	2.539	2.577	2.514	2.520	2.498	2.501	2.516	2.478	0.051
2	2.449	2.419	2.421	2.421	2.406	2.391	2.379	2.384	2.371		
3	2.507	2.504	2.501	2.501	2.534	2.527	2.483	2.499	2.477		
4	2.506	2.490	2.476	2.473	2.484	2.497	2.527	2.550	2.527		
5	2.436	2.416	2.448	2.495	2.509	2.488	2.425	2.437	2.422		

Figure 2: Thickness measurement points and the results.

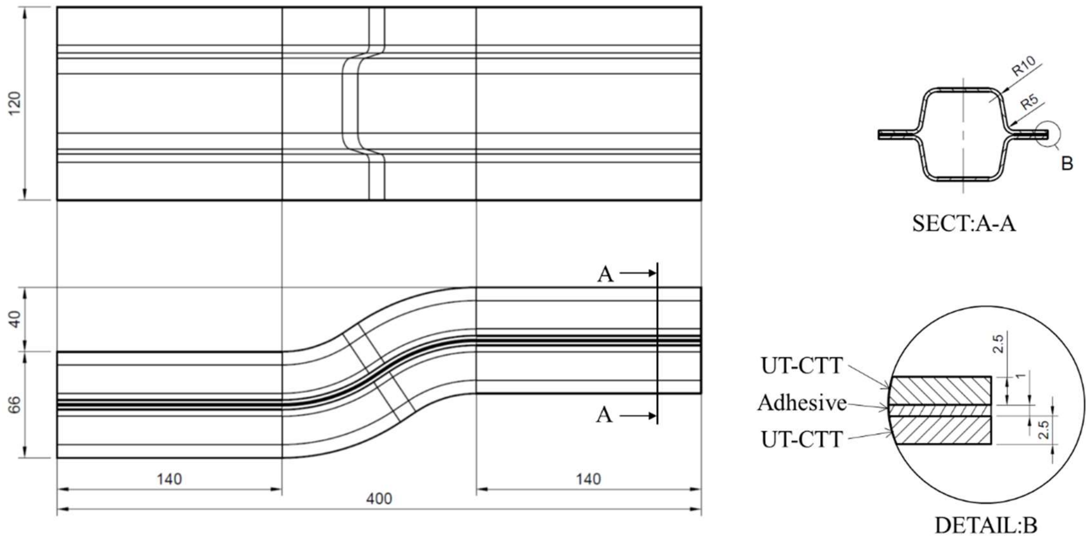

Figure 3: Hollow S-shaped member jointed from two hat-sections.

2.2 Compression Test

Figure 4 shows the compression test overview. Two hollow S-shaped members were placed facing each other, compression tests were carried out on a universal testing machine (AUTOGRAPH AG-250kNXPlus, Shimadzu Co.) at the stroke speed of 1.0 mm/min. The upper and lower 50 mm ends of the hollow S-shaped member were clamped. The cross-sectional view on the Figure 4 (right) shows the clamping method of the hollow S-shaped member. A load wad added to the center of the upper plate on the two members. The displacement of the upper clamp of the left and right members was measured by displacement gauges. The compression test was terminated when left and right imbalance occurred.

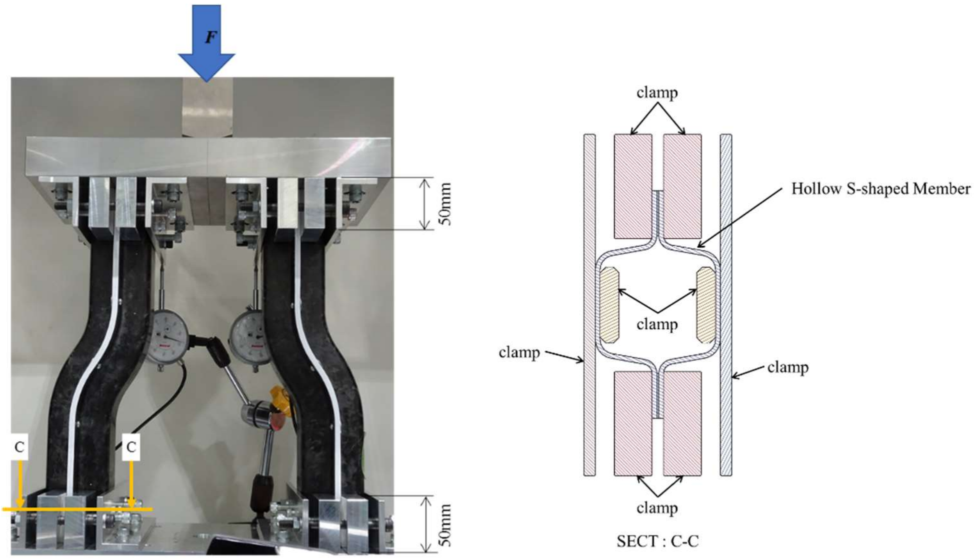

Figure 4: Overview of compression test.

3. FEA METHOD

3.1 FE model and Boundary Conditions

Abaqus/Standard 6.14-5 was utilized for FEA. Figure 5 shows the quarter model. In order to express clamps, the upper and lower ends were defined as rigid bodies. The forced displacement was given to the upper rigid body. CTT and adhesive were solid meshes of hexahedral elements (C3D8), which were connected.

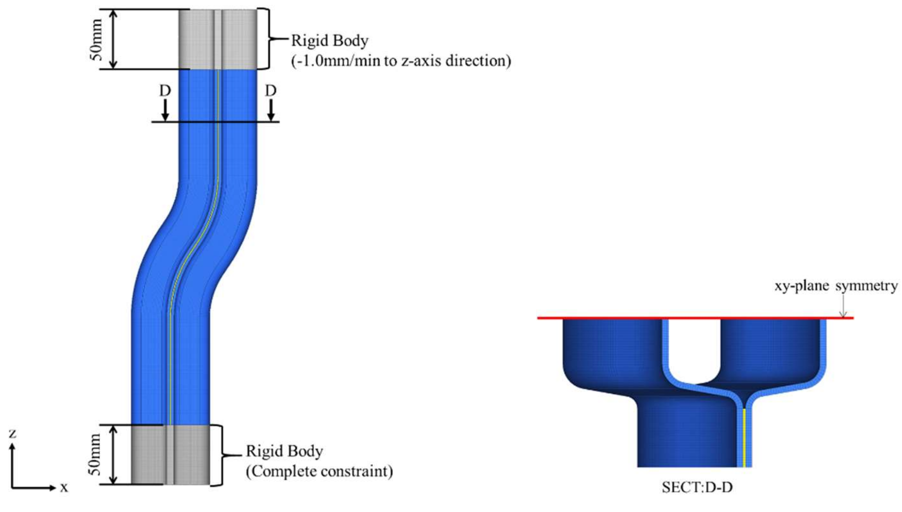

Figure 5: Schematic of hollow S-shaped member FE model.

3.2 Material Parameters

Mechanical properties of BM-CTT and SM-CTT used for FEA are shown in Table 1. And table 2 shows mechanical properties of the adhesive. From the mechanical aspect, BM-CTT and SM-CTT have an in-plane isotropic property. Therefore, it was assumed that $E_1 = E_2$, $\nu_{13} = \nu_{23}$ and $G_{13} = G_{23}$. E_1 and ν_{12} was obtained from the tensile test. It was found that SM-CTT had higher mechanical properties and smaller CV than those of BM-CTT. It is expected to be due to the isotropy of the tape orientation in the tape dispersion process.

E_3 was used by literature value of the Young's modulus E_2 of the unidirectional material in the 90-degree direction. However, any methods for measuring the out-of-plane shear modulus G_{13} has not been established. Yamashita et al. have reported a method to obtain G_{13} from a three-point bending tests [6], but it is difficult to obtain reliable G_{13} because G_{13} of CTT has a high level of scatter. For this reason, in this study we refer to the results of the study by Lyu et al. [7].

Engineering constant	unit	BM-CTT	SM-CTT
ρ		1.50	1.50
$E_1 = E_2$	[GPa]	38.1 (11.7)*	44.8 (5.0)*
E_3	[GPa]	7.33	7.33
$\nu_{12} = \nu_{13} = \nu_{23}$	–	0.24 (26.6)*	0.34 (10.3)*
G_{12}	[GPa]	15.4	16.7
$G_{13} = G_{23}$	[GPa]	4.8	4.8

*Coefficient of Variation

Table 1: Mechanical properties of BM-CTT and SM-CTT.

Engineering constant	unit	MA310
ρ		1.00
E	[GPa]	1.034
ν	–	0.3

Table 2: Mechanical properties of adhesive (MA310).

4. RESULTS AND DISCUSSION

4.1 Experimental Results (BM-CTT)

Figure 6 left shows a typical displacement/load - time curve of BM-CTT. In the first step of the compression test, the left and right members were evenly compressed. In the second step, compressive failure occurred at the carved part of one side, and an imbalance occurred between the right and left displacement. As the compression failure progressed, the adhesive was finally broken. Since the influence of rattling of the test jig was observed just after the compression test started, the tangent line was drawn in the displacement range of 0.3 mm to 0.7 mm, and the intersection point with the x-axis was corrected as the origin (Figure 6 right). At this graph, the slope of the tangent line which is the stiffness of the hollow S-shaped member made by BM-CTT was 74.3 kN/mm.

Whether the right or left member fail depends on the test. Prediction of fracture behaviour is an important research topic, but because of various factors such as tape arrangement and molding condition, it is difficult to predict fracture. For this reason, we focused on the elastic region in this study.

Figure 7 shows the compressive failure at the curved position of the hollow S-shaped member.

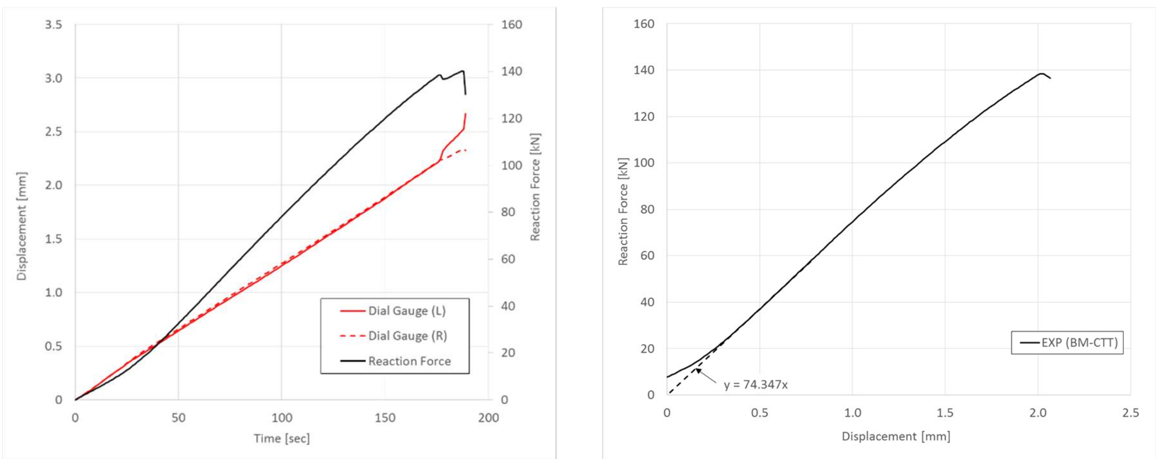

Figure 6: Results of compression test of hollow S-shaped member made by BM-CTT.

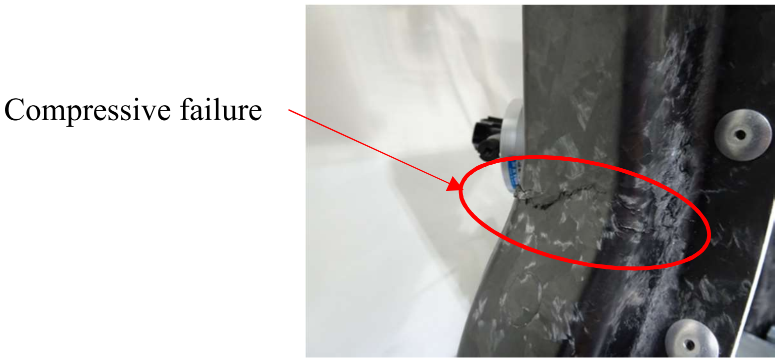

Figure 7: Compressive failure at the curved position of BM-CTT (left member).

4.2 Comparison of FEA results and experimental results (BM-CTT).

Figure 8 (left) shows FEA results of BM-CTT using the average value of the mechanical properties shown in Table 1, and Figure 8 (right) shows simulated results using the values of $\pm 1\sigma$ of E_1 instead of the average value, where σ is the standard deviation. In these figures, the horizontal axis of the curve indicate the average value of the left and right displacement gauges.

In Figure 8 (left), the maximum strength in the experimental results was 138.4 kN at the displacement of 2.02 mm. On the other hand, if we consider CV in E_1 (=E_2), the FEA result were 159.1 kN – 183.4 kN when displaced by 2.02 mm, and the FEA results were about 15% - 39% higher than the experimental results.

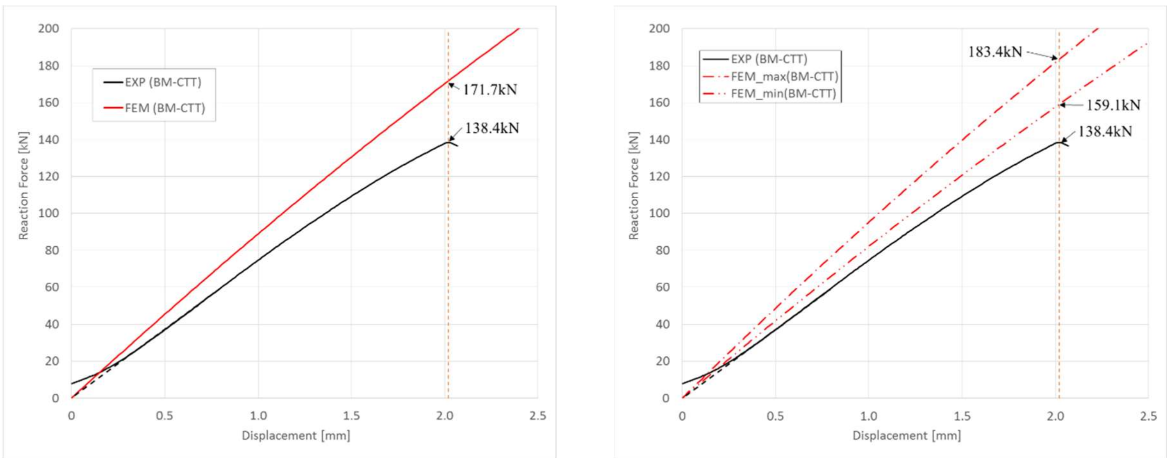

Figure 8: FEM result of BM-CTT.

4.3 Experimental Results (SM-CTT)

Figure 9 (left) shows a typical displacement/load - time curve obtained from the compression test of SM-CTT. In the case of SM-CTT as well as BM-CTT, the left and right member were equally compressed until fracture occurred. Even in the case of SM-CTT, Figure 9 (right) shows that origin correction was carried out by the same methods as BM-CTT. In the case of SM-CTT, the slope of the tangent line which is the stiffness of the hollow S-shaped member was 75.3 kN/mm, and SM-CTT was only 1.3% stiffer than BM-CTT. Figure 10 shows the compressive failure at the curved position of the hollow S-shaped member.

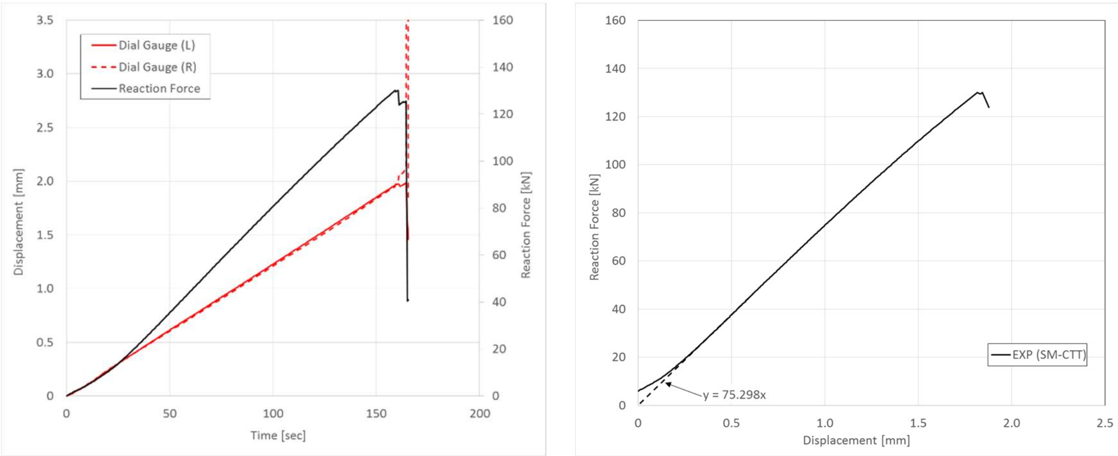

Figure 9: Results of compression test of hollow S-shaped member made by SM-CTT.

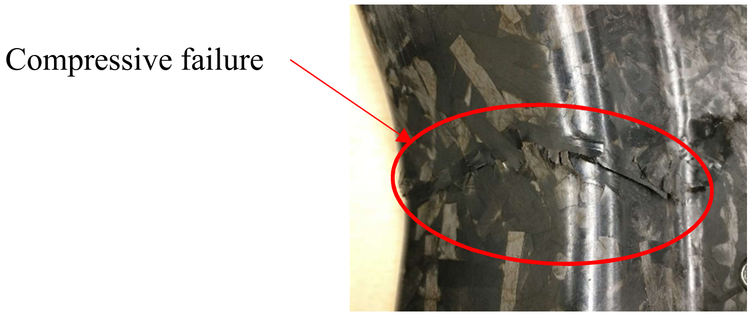

Figure 10: Compressive failure at the curved position of SM-CTT (right member).

4.4 Comparison of FEA results and experimental results (SM-CTT).

Figure 11 shows FEA results of SM-CTT. Figure 11 (left) shows the results calculated by the average value of E_1 (=E_2), and Figure 11 (right) shows the results by the values of $\pm 1\sigma$ of E_1 instead of the average value. The maximum strength in the experimental results was 130.0 kN at the displacement of 1.82 mm.

The FEA result was 169.4 kN – 181.2 kN at 1.82 mm displacement, which was 30% - 39% higher than the experimental result.

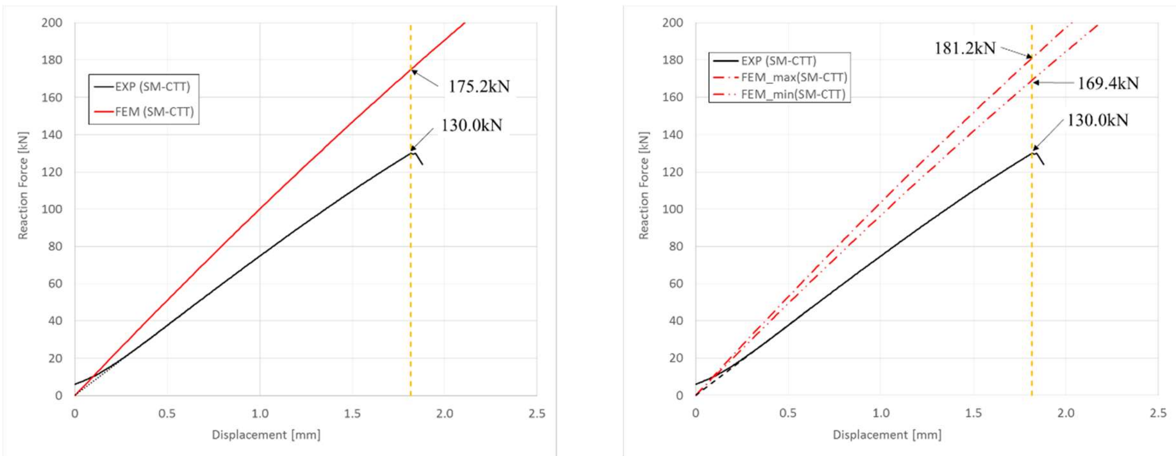

Figure 11: FEM result of SM-CTT.

5. CONCLUSIONS

In this study, we investigated the difference of mechanical properties of hollow S-shaped member using BM-CTT without dispersion process and SM-CTT including air dispersion process.

- The slope of the load-displacement curves, which is the stiffness in the compression test of the hollow S-shaped member, were 74.3 kN/mm for BM-CTT and 75.3 kN/mm for SM-CTT. Although more test results are needed, it is expected that CV due to tape orientation on the member scale is smaller than on the specimen scale.
- In FEA results, even with CV of Young's modulus taken into consideration, they did not match the experimental results. It is inferred that the effect of CV of G_{13} (= G_{23}) needs to be considered in FEA

ACKNOWLEDGEMENTS

Part of this research was conducted as Japanese METI Project "The Future Pioneering Projects / Innovative Structure Materials Project" since 2013fy. Authors would like to express sincerely appreciation to the project members who have provided valuable information and useful discussions. In especially, Industrial Technology Center of Fukui Prefecture, Fukui Fibertech co., Ltd. and KADO co. deeply committed preparation of S-shaped member.

REFERENCES

[1] T. Ohori, T. Hayashi and J. Takahashi, "FEA Using Design Optimization Technique for an Application of Carbon Fiber Reinforced Thermoplastics to Automobile Body Structure", *Proceedings of the 20th International Conference of Composite Materials*, *Copenhagen, Denmark, July 19-24, 2015*.

[2] P. Feraboli, E. Peitso, F. Deleo and T. Cleveland. Characterization of prepreg-based discontinuous carbon fiber/epoxy systems. *Journal of reinforced plastics and composites*, **28**, 2009, pp. 1191-1214.

[3] M. Selezneva and L. Lessard. "Characterization of mechanical properties of randomly oriented strand thermoplastic composites". *Journal of composite materials*, **50**, 2016, pp. 2833-2851.

[4] M. Selezneva, S. Roy, L. Lessard and A. Yousefpour. "Analytical model for prediction of strength and fracture paths characteristic to randomly oriented strand (ROS) composites". *Composites Part B*, **96**, 2016, pp. 103-111.

[5] H. Suganuma, S. Yamashita, X. Zhang, K. Hashimoto, I. Ohsawa and J. Takahashi, "Influence of dispersion method to dispersibility and mechanical properties of ultra-thin carbon fiber tape reinforced thermoplastics", *Proceedings of the 20th International Conference of Composite Materials*, *Copenhagen, Denmark, July 19-24, 2015*.

[6] S. Yamashita, I. Ohsawa, T. Matsuo, X. Zhang and J. Takahashi, "Evaluation of Young's Modulus and Out-of-Plane Shear Modulus of Carbon Fiber Reinforced Thermoplastics by Three Point Bending Test", *J Jpn Soc Compos Mater*, **39**, 2013, pp.221-230.

[7] X. Lyu, J. Takahashi, Y. Wan and I. Ohsawa, "Determination of transverse flexural and shear moduli of chopped carbon fiber tape-reinforced thermoplastic by vibration", *Journal of Composite Materials,* accepted, (DOI: 10.1177/0021998317707815)